Chapter 16

Microthermomechanical Probing of Thin Composite Polymer Films

Vladimir V. Tsukruk, Valery Gorbunov, Igor Luzinov, Zheng Huang, and Nobi Fuchigami

Department of Materials Science and Engineering, Iowa State University, Ames, IA 50011

Surface distribution of micromechanical properties of polystyrene-polybutadiene (PS/PB) thin films is probed in the range of temperatures. We demonstrate that for heterogeneous polymer films, the micromapping of surface properties can be obtained *concurrently* for glassy and rubber phases as well as across the interface. The histogram of the surface distribution of elastic modulus display two very distinctive maxima for glassy and rubber phases at 2.5 GPa and 6 MPa, respectively. The depth profile measurements demonstrate consistent changes of the rubber phase thickness with distance from the PS/PB interface. Glass transition temperature of glassy matrix, flow temperature of rubber phase, and difference in thermal conductivities all can be collected for heterogeneous polymer films on a microscopic scale.

Introduction

First attempts to record the micro/nanomechanical surface properties with atomic force microscopy/scanning probe microscopy (AFM/SPM) probing were conducted by using the classical Sneddon's approach [1-3]. Further development lead to the micromapping of the surface mechanical properties with a force modulation mode [4-8]. Several studies were focused on the development of dc force-displacement probing of the micromechanical properties [9-15]. In this communication, we report on studies of the micromechanical properties of composite films of polystyrene/polybutadiene (PS/PB) and grafted PS layers and prove the feasibility of

In Interfacial Properties on the Submicrometer Scale; Frommer, Jane, et al.;
ACS Symposium Series; American Chemical Society: Washington, DC, 2000.

of force-displacement data collection/analysis approach to obtain reliable micromechanical data for composite materials.

Experimental

Samples for investigation were prepared by spin-coating of polystyrene (M_w = 250, 000, Janssen Chemical Co.) / polybutadiene (M_w = 420, 000, Aldrich) blends on a silicon wafer with PS as a glassy matrix and PB as a dispersed rubber phase. The film thickness was kept within 2 - 5 μm. Composite films were probed with a Dimension 3000 microscope (Digital Instruments) in a Force Volume mode with 2 Hz probing frequency and a lateral resolution 32 x 32 or 64 x 64 pixels. Scan sizes varied from 2 x 2 m to 30 x 30 m. The DI thermal stage was used for data collection in the range of temperatures up to 120°C. The SPM tips were silicon tips with a spring constant determined by a combination of resonant frequency measurements and spring-against-spring techniques *(16-18)*. We measured the cantilever resonance frequency and estimated normal and torsional spring constants from calibration plots proposed earlier *(17)*. Tip radius was measured by scanning gold nanoparticles chemically attached to self-assembled monolayers and using a spherical approximation to extract parameters from cross-sections *(19)*.

For data processing, we used the protocol for the microprobing of the adhesive forces and elastic modulus based on the contact model of elastic deformation modified for SPM measurements *(12, 13, 15)*. We analyzed repulsive part of approaching force-distance curves and used the Hertzian contact mechanics model (sphere against plane) combined with the two-spring model to evaluate elastic modulus from these force-distance data. No viscoelastic contribution was taken into account in current analysis. This approach was proved reliable for the probing the range of polymeric materials with elastic modulus as low as 1 MPa and as high as 3 GPa *(12-15)*. The focus of this study was on finding optimal parameters for *concurrent* collection of micromechanical data for two phases (rubber and glassy) with very different elastic properties. Scanning thermal imaging was performed according to the procedure discussed before *(20, 21)* on an Explorer microscope (Thermomicroscopes).

Results and discussion

As was observed, all PS/PB films are highly heterogeneous with well-developed microphase separation of rubber and glassy phases (Figure 1). The lateral size of the dispersed rubber phase varies from 20 μm to less than 1 μm. Rubber inclusions form either depleted or elevated round-shaped droplets. Cracks are occasionally observed to originate at the rubber-glass interface and propagate through the glassy matrix between large rubber droplets (Figure 1).

In Interfacial Properties on the Submicrometer Scale; Frommer, Jane, et al.;
ACS Symposium Series; American Chemical Society: Washington, DC, 2000.

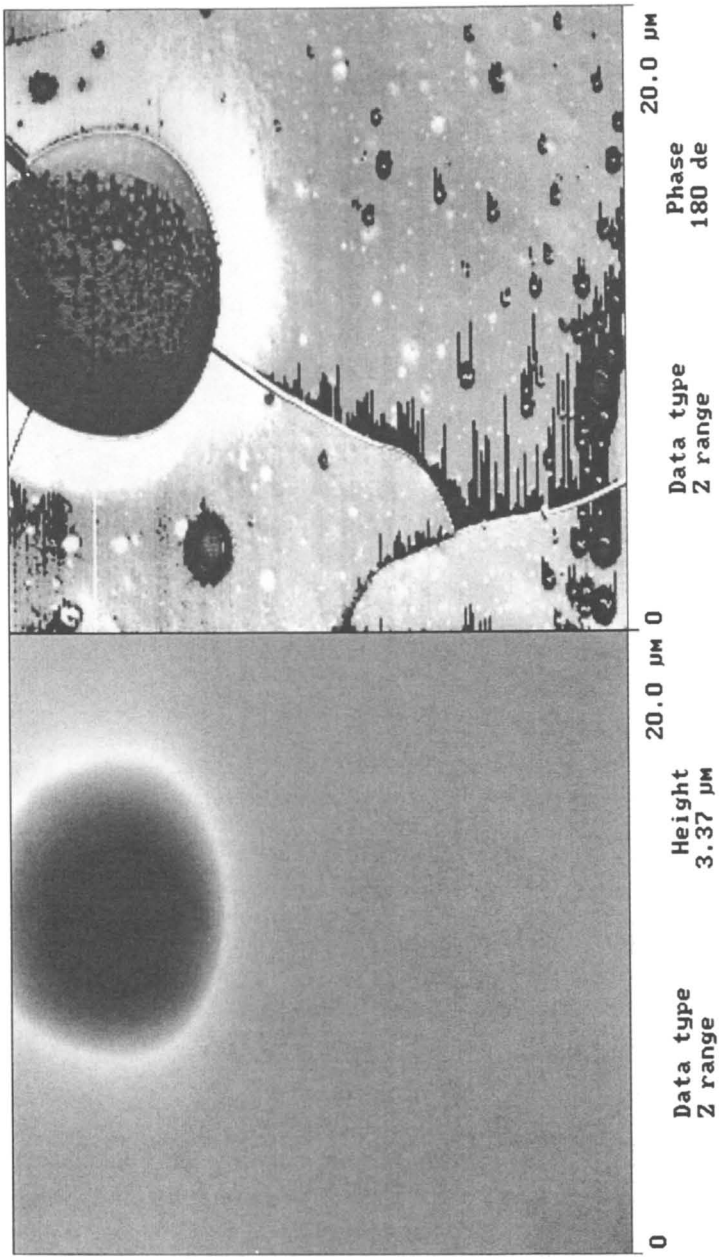

Publication Date: December 18, 2000 | doi: 10.1021/bk-2001-0781.ch016

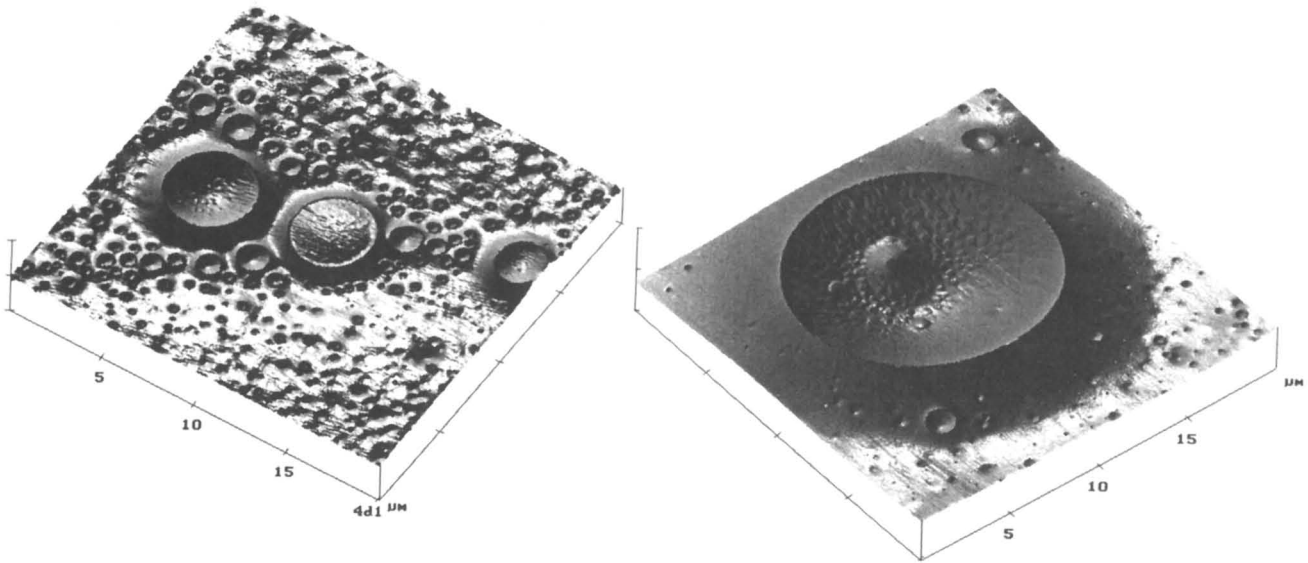

Figure 1. Topography of the PS/PB film with PB as the dispersed rubber phase. Pay attention to the dimensional variation of the PB droplets and the presence of the PS microinclusions inside a large rubber droplet. Top: topography (left) and phase (right) images of the same surface area. Bottom: 3-D representation of the polymer surface at two different locations.

In Interfacial Properties on the Submicrometer Scale; Frommer, Jane, et al.;
ACS Symposium Series; American Chemical Society: Washington, DC, 2000.

Figure 2 demonstrates the micromapping data (topography, elastic modulus, and adhesive forces) obtained concurrently for the same surface area of the composite film. It shows that, for the rubber phase, the adhesive forces are much higher and elastic modulus is much lower as compared to the glassy matrix. The histogram of the surface distribution of elastic moduli displays two very distinctive peaks (Figure 2). The first, very sharp peak is located in the range 3 - 10 MPa and corresponds to the rubber phase. The broad distribution of elastic moduli between 2 - 4 GPa corresponds to the PS matrix.

Absolute values obtained by the SPM probing are very close to those expected for the bulk material (2-3 MPa for PB and 2-3 GPa for PS) [8]. The higher average value of elastic modulus observed for rubber phase within microscopic droplets can be related to its confined state in the form of thin layers and droplets, a relatively short probing time, as well as the presence of some PS microinclusions inside large rubber droplets (Figure 1). On the other hand, a broad distribution and lower value of elastic modulus for the PS matrix are caused by multiple defects in the form microcracks and small inclusions of rubber phases. A cross-section of the PB phase allows observing close correlation among surface properties as shown in Figure 3. As clear from this data, adhesion and elasticity follow closely topography with sharp changes across the rubber-glass interface, which occupies a fraction of a micrometer in a lateral direction.

Microprobing technique applied here is sensitive to the depth distribution of the elastic properties and can provide insight on buried details of the surface distribution of different polymer phases. As demonstrated in Figure 4, elastic modulus for the rubber phase shows the presence of hard PS surface underneath of compliant material. The elastic modulus depth profile shows a large variation at a very low indentation depth (below 20 nm) caused, mainly, by the instability of the first mechanical contact as discussed in our previous papers [12-14]. In the range of indentation depths from 20 to 150 nm, a gradual decrease of elastic modulus is observed that can be related to either surface hardening phenomena or rate dependent (viscoelastic) contribution. At intermediate indentation depth, a stable, virtually constant value of the elastic modulus is recorded.

For various rubber droplets, a sharp increase of elastic modulus takes place at a very high indentation depth, far exceeding the limitations of the Hertzian model (Figure 4). Therefore, absolute values in this indentation range should be treated with care and here we discuss only qualitative behavior. A sharp increase of "apparent" elastic modulus at higher indentation depths can be associated with the tip approaching a hard PS surface below the rubber phase. Indeed, we observed a significant variation of this depth from 100 nm in the vicinity of the rubber-matrix interface and within very small (less than a micrometer diameter) rubber droplets to as large as >800 nm in the central part of large rubber particles (Figures 4, 5). This depth approximately corresponds to the expected thickness of rubber droplets of different lateral sizes as illustrated in Figure 5 and indicates that rubber material is virtually completely compressed under the SPM tip. Therefore, we conclude that the sharp increase of elastic response at high indentation depth detected by the SPM tip indicates the thickness of the rubber layer on a top of the glassy matrix at a particular location.

At the elevated temperature, the micromapping of composite films shows distinctive rubber and glassy phases up to 100°C. At even higher temperatures, adhesion and elastic surface distributions become very homogeneous with no detectable differences in the micromechanical properties detected between PS and PB phases (Figure 6). Sharp deviations observed only along the rim of round inclusions (the width is less than one micrometer) are caused by the geometrical contribution of different elevations at the PB-PS interface.

From the micromapping data obtained at different temperatures, we measured the temperature dependence of elastic modulus separately for glassy and rubber phases (Figure 7). The absolute value of elastic modulus for the PS phase is virtually constant (about 2 GPa) within an interval of temperatures from room temperature to about 100°C. A sharp drop of PS elastic modulus to the value below 10 MPa is observed within a narrow temperature interval from 100 to 120°C. This indicates glass transformation (103°C as measured by DSC for this PS) and the transition of the glassy matrix to the elastic state.

On the other hand, the average elastic modulus of the rubber phase decreases steadily for higher temperatures (up to 100°C) (Figure 7). Then, its value increases sharply around 110°C and decreases again. This behavior can be understood after careful analysis of modulus depth profiles. Indeed, we estimated the elastic modulus by averaging over a complete indentation depth interval. At temperatures higher than the flow temperature of the PB phase (100°C), the SPM tip penetrates through the viscous phase and effectively interacts only with the hard PS surface. This results in sharp increase of the "integrated" elastic modulus value, which is, essentially, PS modulus itself at this temperature. At even higher temperature, the PS matrix goes through transformation to the elastic state that manifests itself in the sharp reduction of integrated elastic modulus to typical rubber level.

Scanning thermal microscopy (SThM) was used to estimate the surface distribution of the microthermal properties (for details see Ref. 21). As can be seen from the images obtained in this mode (Figure 8, substantial thermal contrast for PB and PS phases can be detected at the probe temperature above 50°C. A geometrical contribution is also clearly visible However, taking into account that the effective thermal contact area for polymeric materials is about 1 μm [21], we can refer the major contribution in different thermal response for the polymer film to different thermal conductivities of glassy and rubber phases.

Finally, we tested micromechanical properties of ultrathin, monomolecular PS brushes with the thickness of 8 nm (determined by ellipsometry and AFM) [22]. The polymer layer is chemically tethered to the surface and posses molecularly smooth surface morphology (Figure 9). We performed micromapping around a worn area intentionally produced by the previous scanning with high forces (Figure 10). We observed that the elastic modulus value inside the worn area (a bare silicon surface) and on the intact PS brush layer exceeds the upper measurable limit of our experimental set-up (10 GPa in this case). This indicates that the SPM tip penetrated completely through the compliant polymer brush layer and probed the underlying silicon surface. Elastic modulus of polymer debris around the worn area was measured to be in the range 300 MPa - 1 GPa, which is fairly close to the expected value for low molar mass PS material. This example demonstrates that microprobing

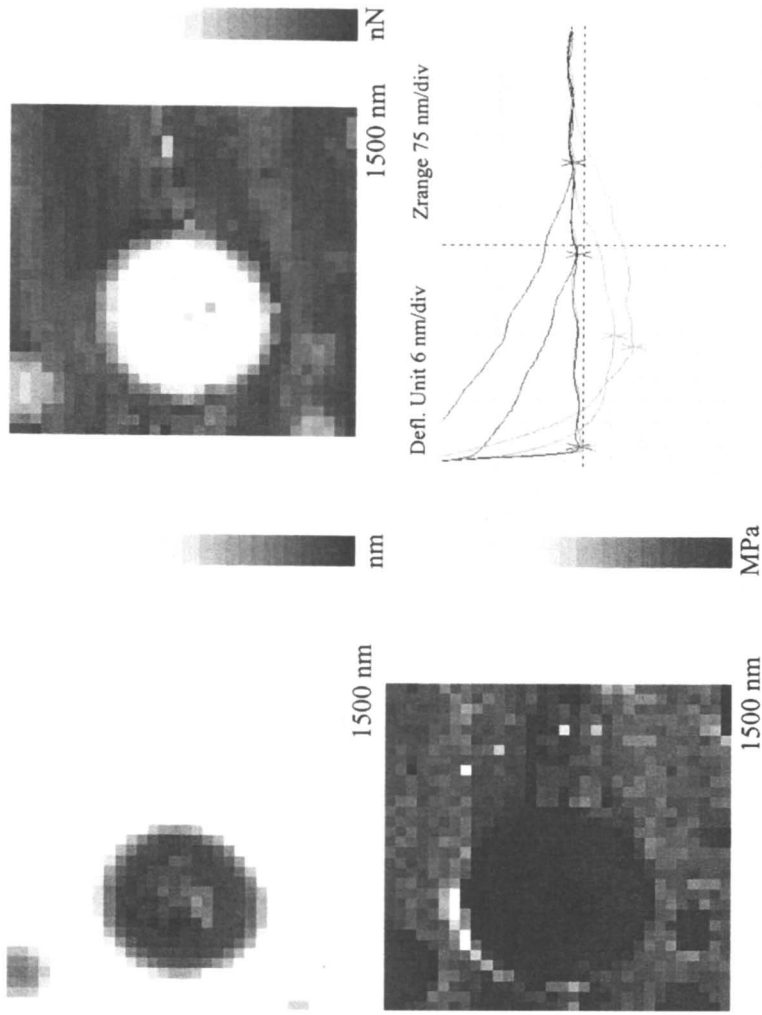

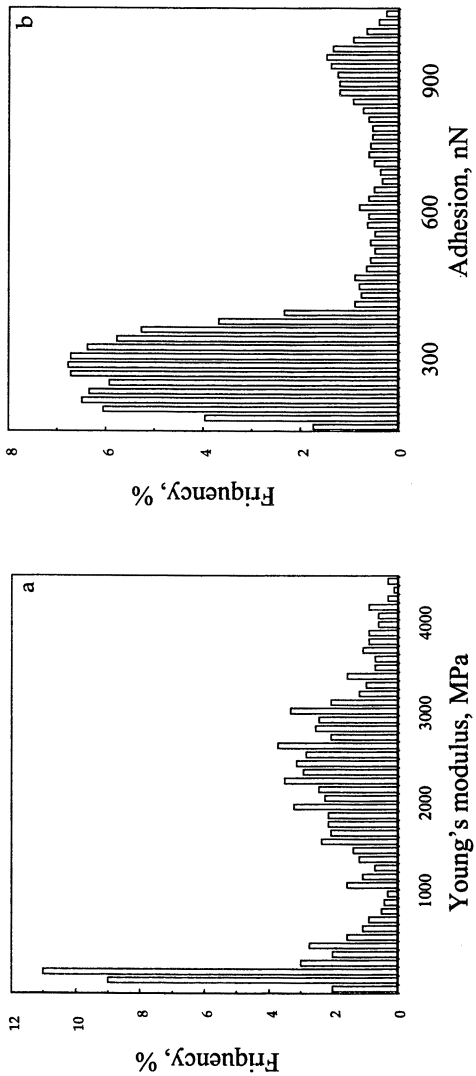

Figure 2. Top: topography (left top), adhesion (right top), and elastic modulus (left bottom) images of the PS/PB blend (15 x 15 μm). Force-distance curves are shown for rubber and glassy phases (right bottom). All mappings are done with the 64 x 64 pixel lateral resolution. Two histograms (bottom) of elastic modulus distribution and adhesive forces show two distinctive peaks for rubber and glassy phases.

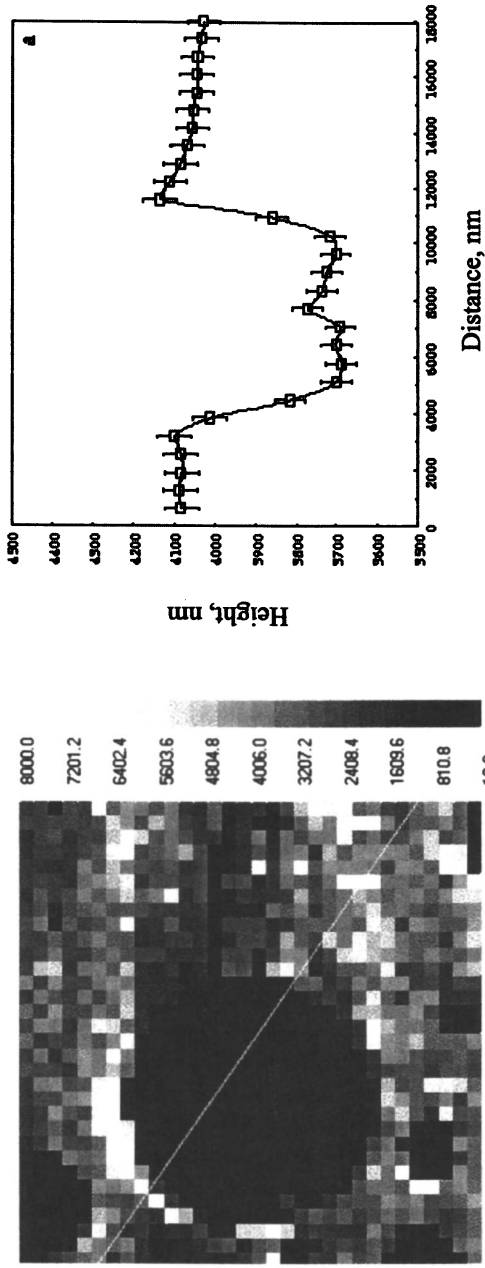

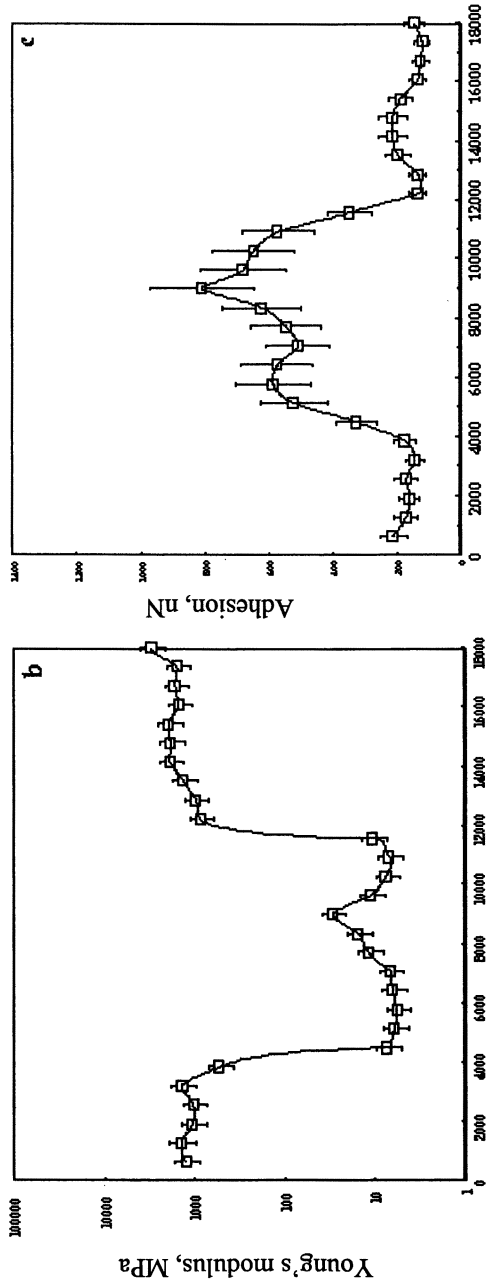

Figure 3. Cross-sections of the rubber phase surface properties within the glassy matrix: elastic modulus, adhesive force, and topography variation are recorded and calculated along the line shown on the image.

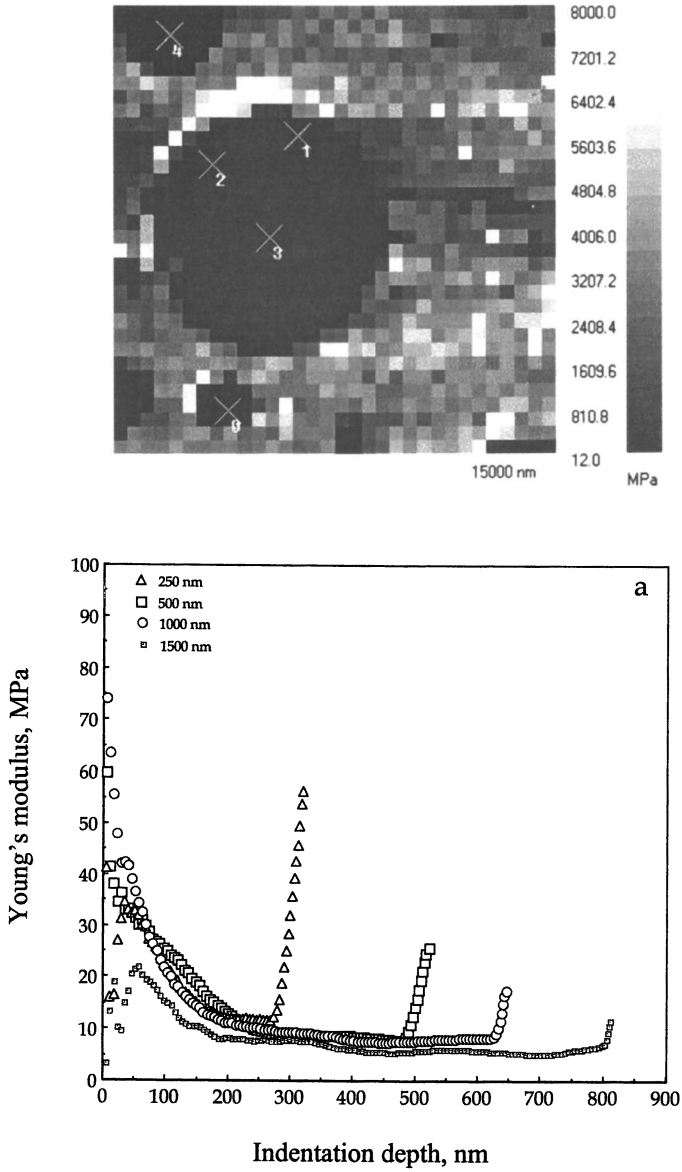

Figure 4. The depth profile of elastic moduli for the rubber phase at different locations within the large rubber droplet and within smaller rubber droplets, numbers indicate the distance from the glassy-rubber interface.

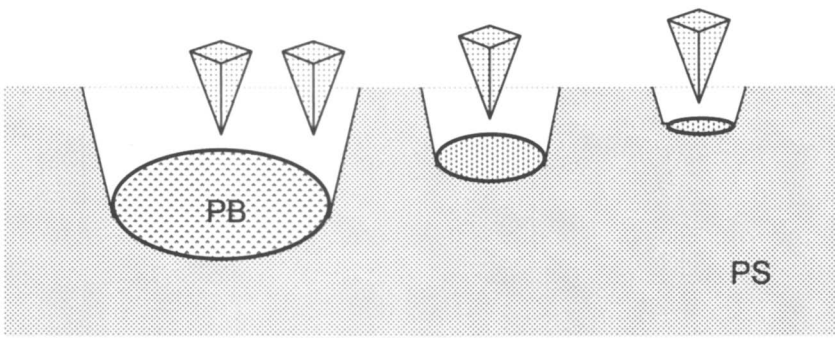

Figure 5. Schematic representation of the micromechanical probing of the rubber droplets with different diameter/thicknesses. Four locations correspond to depth profiles presented in Figure 4.

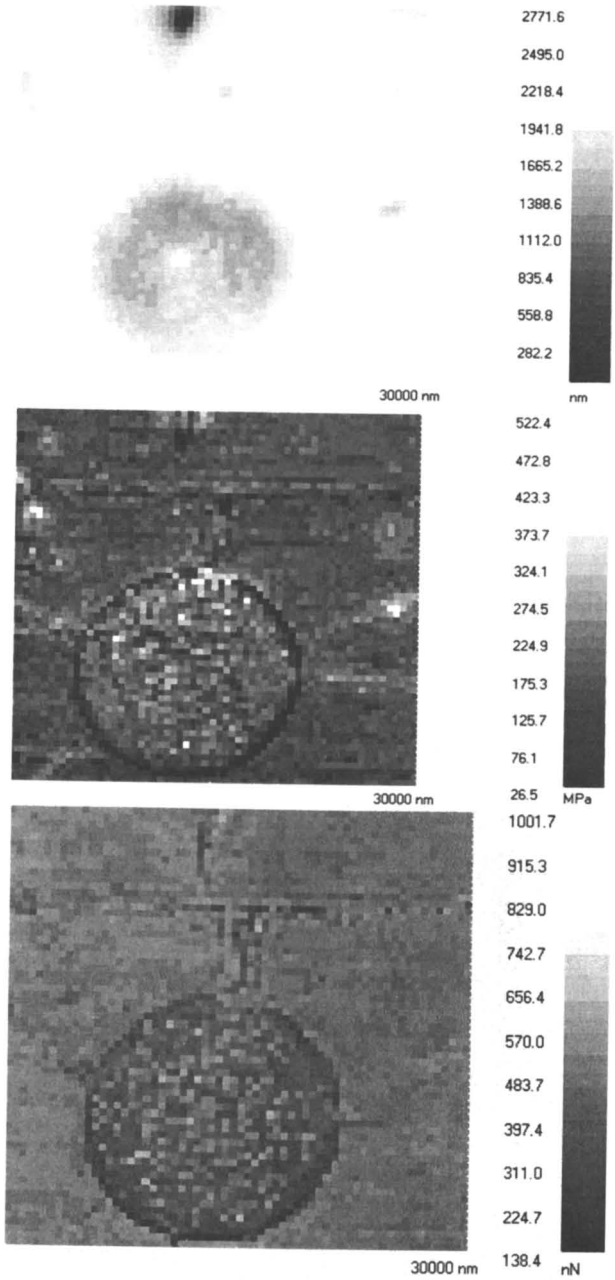

Figure 6. The microprobing of the polymer composite film at elevated temperatures. Topography (top), elastic modulus (middle), and adhesion (bottom), images of PS/PB film (30 x 30 μm) obtained at 120°C. Pay attention to the homogeneous surface distribution of elastic and adhesive properties except the geometrical contribution across the PS/PB interface.

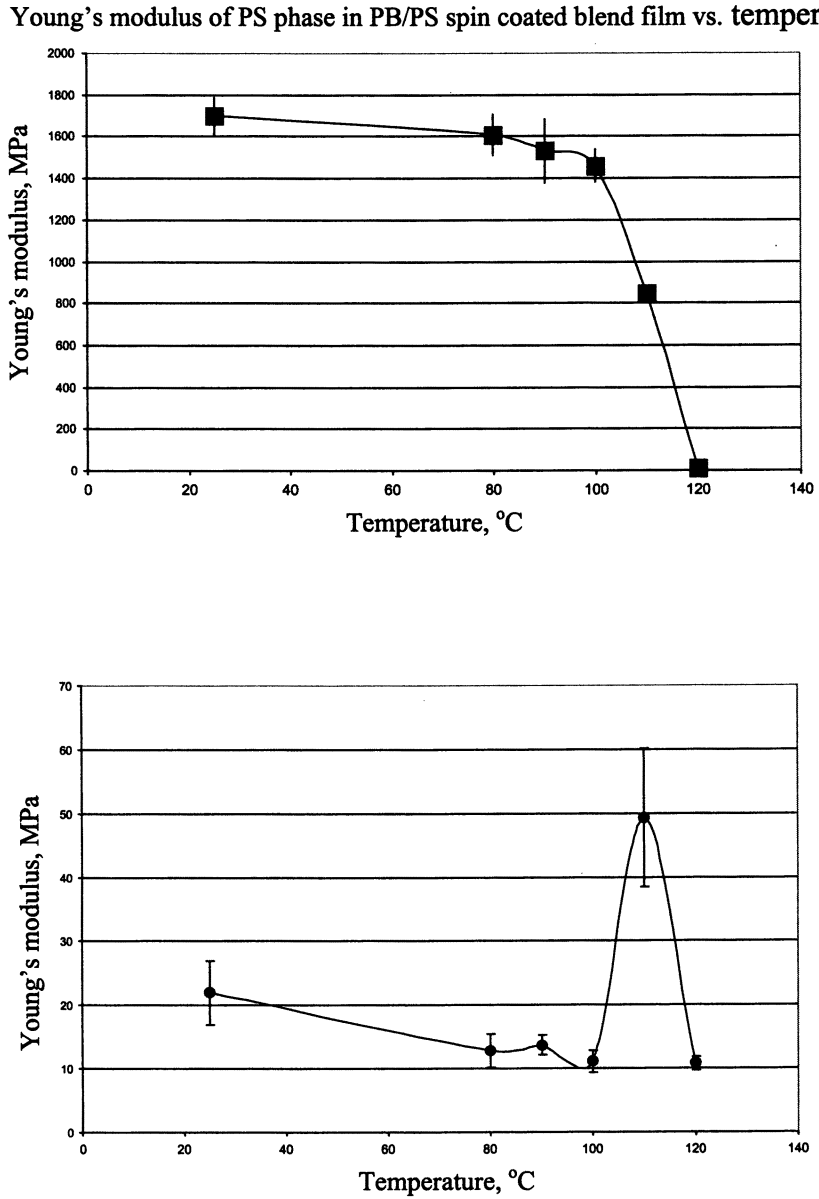

Figure 7. Temperature variation of elastic modulus for the PS matrix (top) and the rubber phase (bottom) as derived from the surface histogram.

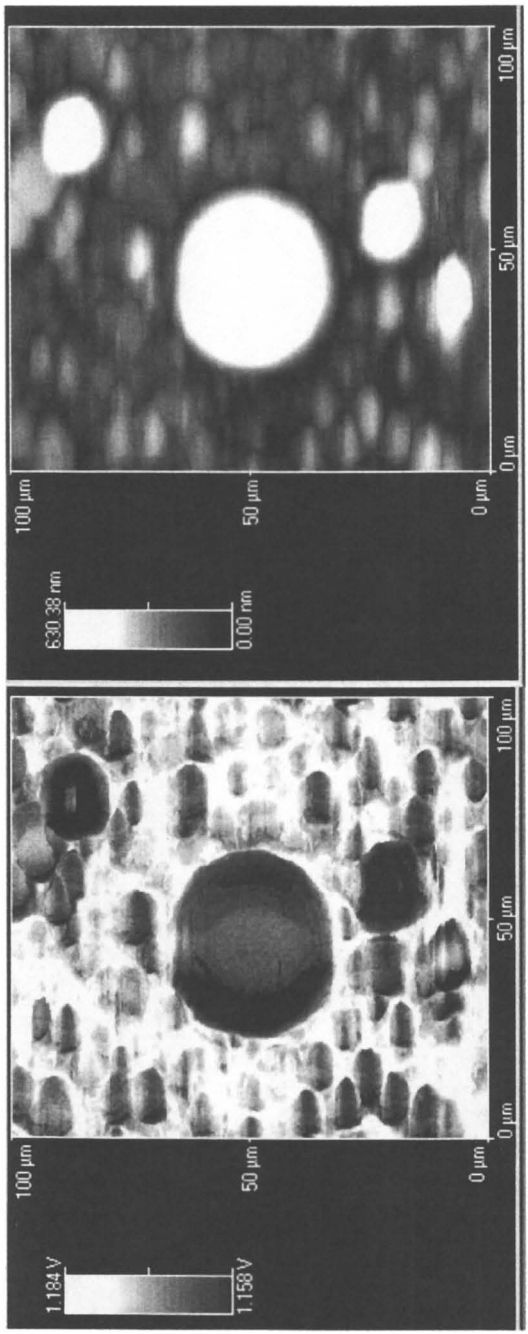

Figure 8. Topography and thermal images of the PS/PB film obtained by the SThM mode at the probe temperature of 60°C.

Publication Date: December 18, 2000 | doi: 10.1021/bk-2001-0781.ch016

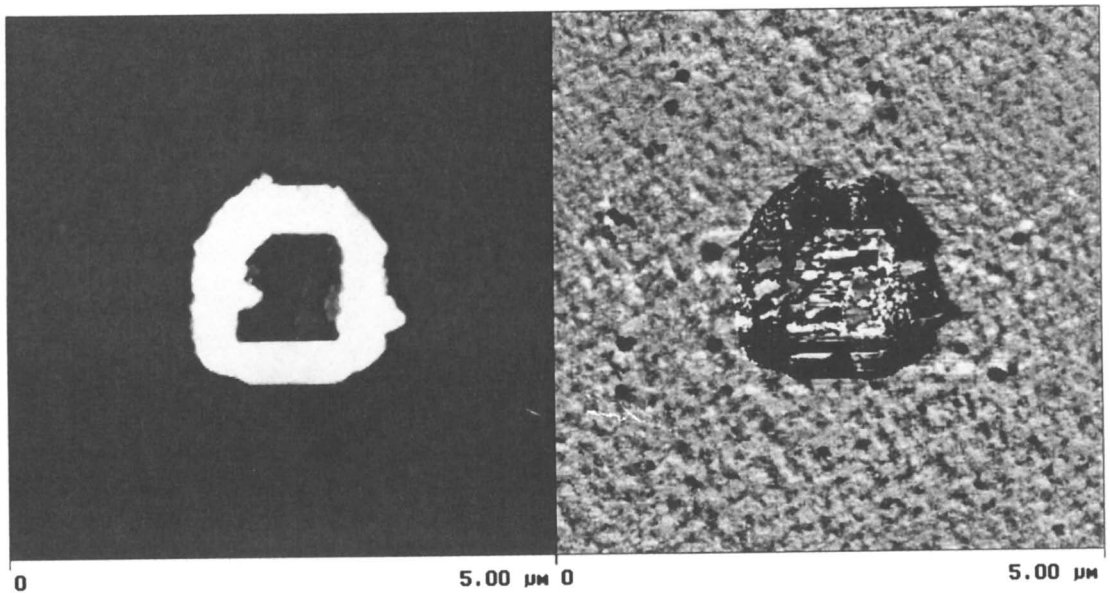

Figure 9. Topography (left) and phase image (right) of PS molecular layer (8 nm thick) tethered to a silicon wafer with the worn area produced by selective scanning with high forces (scan size: 5 x 5 µm).

In Interfacial Properties on the Submicrometer Scale; Frommer, Jane, et al.; ACS Symposium Series; American Chemical Society: Washington, DC, 2000.

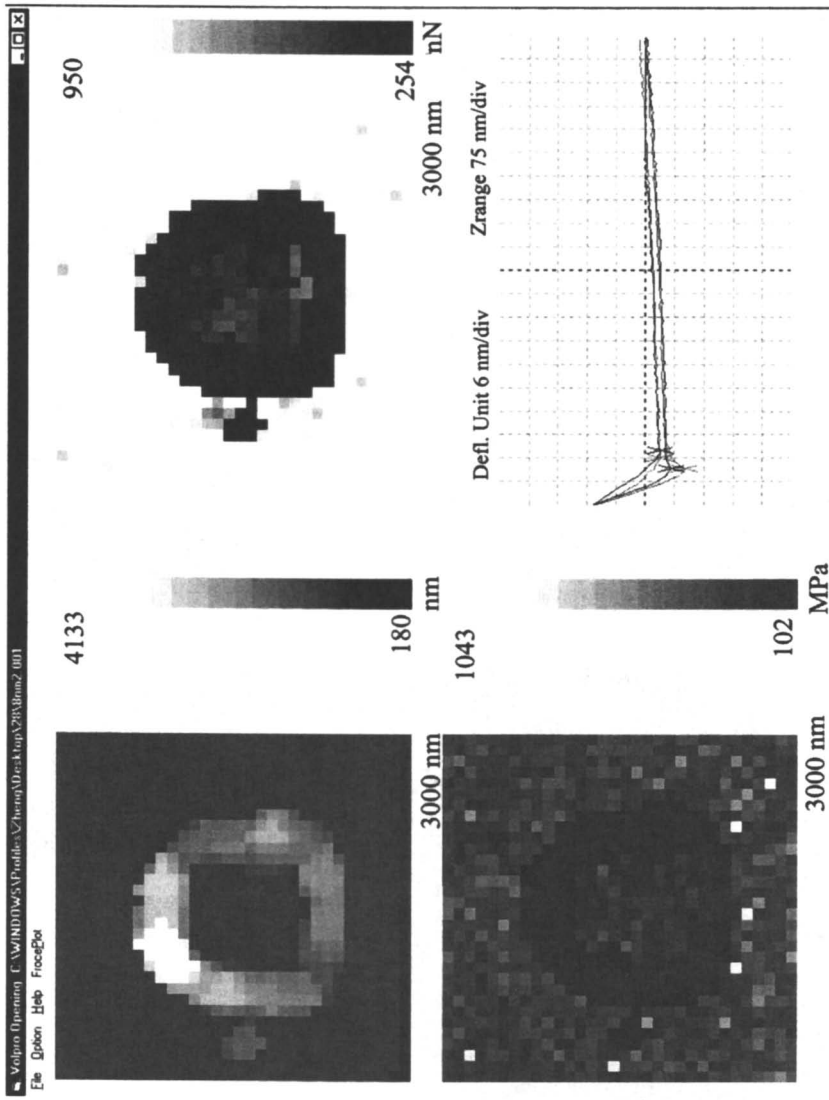

Publication Date: December 18, 2000 | doi: 10.1021/bk-2001-0781.ch016

Figure 10. The microprobing of polymer molecular layer chemically tethered to a silicon wafer. Topography (left top), adhesion (right top), and elastic modulus (left bottom) images of the film (3 x 3 μm) with the worn area along with the example of force-distance curves (right bottom). Data shows low adhesion in the debris area and within the worn area and lower elastic modulus for polymer debris.

In Interfacial Properties on the Submicrometer Scale; Frommer, Jane, et al.;
ACS Symposium Series; American Chemical Society: Washington, DC, 2000.

technique explored in our work can be very informative for extremely thin polymer layers, down to a monomolecular layer.

Acknowledgment

This work is supported by The Surface Engineering and Tribology Program, The National Science Foundation, CMS-9996445 Grant and AFOSR F49620-93-C-0063 Contract. The authors thank Dr. S. Chizhik for assistance and discussions.

References

1. Binnig, G., Quate, C.F. and Gerber, Ch. *Phys. Rev. Lett.* **1986**, *12*, 930.
2. Landman, U., Luedtke, W. D., Burnham, N. A. and Colton, R. J. *Science,* **1990**, *248*, 454.
3. Burnham, N. A. and Colton, R. J. *J. Vac. Sci. Technol.,* **1989**, *A7*, 2906.
4. Oulevey, F., Gremaud, G., Semoroz, A., Kulik, A. J., Burnham, N. A., Dupas, E. and Gourdon, D. *Rev. Sci. Instr.,* **1998**, *69*, 2085.
5. Marti, O. and Hild. S. in: *Microstructure and Microtribology of Polymer Surfaces,* eds. V. V. Tsukruk, K. Wahl, ACS Symposium Series, v. 741, 2000, p.212.
6. Radmacher, M., Tillmann, R. W. and Gaub, H. E. *Biophys. J.,* **1993**, *64*, 735.
7. Kajiyama, T., Tanaka, K. and Takahara, A. *Macromolecules,* **1997**, *30*, 280.
8. Aklonis, J. J. and MacKnight, W. J. *Introduction to Polymer Viscoelasticity,* J. Wiley & Sons: NY, 1983.
9. Vanlandingham, M. R., McKnight, S. H., Palmese, G. R., Ellings, J. R., Huang, X., Bogetti, T. A., Eduljee, R. F. and Gillespie, J. W. *J. Adhesion,* **1997**, *64*, 31.
10. Overney, R. and Tsukruk, V. V. in: *Scanning Probe Microscopy of Polymers,* eds. B. Ratner and V. V. Tsukruk, ACS Symposium Series, 1998, v. 694, p. 2.
11. Domke, J. and Radmacher, M. *Langmuir,* **1998**, *14*, 3320.
12. Chizhik, S. A., Huang, Z., Gorbunov, V. V., Myshkin, N. K. and Tsukruk, V. V. *Langmuir*, **1998**, *14,* 2606.
13. Tsukruk, V. V., Huang, Z., Chizhik, S. A. and Gorbunov, V. V. *J. Materials Science,* **1998**, *33,* 4905.
14. Huang, Z., Chizhik, S. A., Gorbunov, V. V., Myshkin, N. K. and Tsukruk, V. V. in: *Microstructure and Microtribology of Polymer Surfaces,* Eds. V. V. Tsukruk, K. Wahl, ACS Symposium Series, v. 741, 2000, p. 177.
15. Tsukruk, V. V., Gorbunov, V. V., Huang, Z., Chizhik, S. A. *Polym. Intern.* 1999, accepted
16. Hazel, J. L. and Tsukruk V. V. *J. Tribology,* **1998**, *120,* 814.
17. Hazel, J. L. and Tsukruk, V. V. *Thin Solid Films*, **1999**, *339,* 249.
18. Huang, Z. *MS Thesis*, Western Michigan University, 1999.

19. Bliznyuk, V. N., Hazel, J. H., Wu, J. and Tsukruk, V. V. in: *"Scanning probe Microscopy of Polymers",* Eds. B. Ratner, V. V. Tsukruk, 1998, v. 694, p. 252
20. Hammiche, A., Hourston, D. J., Pollock H. M., Reading, M., Song, M. *J. Vac. Sci. Techn.,* **1996**, *14(2),* 1486.
21. Gorbunov, V. V., Fuchigami, N., Hazel, J. L., Tsukruk, V. V. *Langmuir,* **1999,** *15,* 8340.
22. Luzinov, I., Julthongpiput, D., Malz, H., Pionteck, J., Tsukruk, V. V. *Macromolecules,* 1999, accepted